

1-22-2021

## Analytical solution of startup critical hydraulic gradient of fine particles migration in sandy soil

Ming-nian WANG

*Key Laboratory of Transportation Tunnel Engineering of Ministry of Education, Southwest Jiaotong University, Chengdu, Sichuan 610031, China*

Yong-tao JIANG

*Key Laboratory of Transportation Tunnel Engineering of Ministry of Education, Southwest Jiaotong University, Chengdu, Sichuan 610031, China*

Li YU

*Key Laboratory of Transportation Tunnel Engineering of Ministry of Education, Southwest Jiaotong University, Chengdu, Sichuan 610031, China, yuli\_1026@home.swjtu.edu.cn*

Yu-cang DONG

*Key Laboratory of Transportation Tunnel Engineering of Ministry of Education, Southwest Jiaotong University, Chengdu, Sichuan 610031, China*

*See next page for additional authors*

Follow this and additional works at: <https://rocksoilmech.researchcommons.org/journal>



Part of the [Geotechnical Engineering Commons](#)

---

### Custom Citation

WANG Ming-nian, JIANG Yong-tao, YU Li, DONG Yu-cang, DUAN Ru-yu, . Analytical solution of startup critical hydraulic gradient of fine particles migration in sandy soil[J]. Rock and Soil Mechanics, 2020, 41(8): 2515-2524.

This Article is brought to you for free and open access by Rock and Soil Mechanics. It has been accepted for inclusion in Rock and Soil Mechanics by an authorized editor of Rock and Soil Mechanics.

---

# Analytical solution of startup critical hydraulic gradient of fine particles migration in sandy soil

## Authors

Ming-nian WANG, Yong-tao JIANG, Li YU, Yu-cang DONG, and Ru-yu DUAN

## Analytical solution of startup critical hydraulic gradient of fine particles migration in sandy soil

WANG Ming-nian<sup>1,2</sup>, JIANG Yong-tao<sup>1,2</sup>, YU Li<sup>1,2</sup>, DONG Yu-cang<sup>1,2</sup>, DUAN Ru-yu<sup>1,2</sup>

1. School of Civil Engineering, Southwest Jiaotong University, Chengdu, Sichuan 610031, China

2. Key Laboratory of Transportation Tunnel Engineering of Ministry of Education, Southwest Jiaotong University, Chengdu, Sichuan 610031, China

**Abstract:** Suffusion will occur in the internally unstable sandy soil because of the groundwater seepage. Soil failure caused by the suffusion has adverse effects on the building structures or foundations. In this paper, a model that can calculate the force acted on fine particles in seepage field was established by considering the effective stress of soil and the stress reduction of fine particles. According to the equilibrium state of ultimate stress, the formula for calculating the startup critical hydraulic gradient of fine particles migration in sandy soil during the suffusion process was obtained. A DEM-CFD coupled method and the existing experimental data were used to validate the proposed model. The results showed that the fine particles in the sandy soil started in rolling mode in the beginning, and the startup critical hydraulic gradient is found to be affected by the seepage flow, soil characteristics, and the properties of the particles. The startup critical hydraulic gradient of fine particles on the surface of sandy soil was found greatly affected by the buried depth. The difference between the highest and lowest startup critical hydraulic gradient of the fine particles buried in 1 cm depth was 10.169%, and the difference was reduced to 1.061% when the buried depth was 10 cm. The maximum standard error of the calculation method was 6.038% while compared to the numerical simulation results, the maximum standard error compared to the seepage test results was 11.211%. Therefore, the proposed model can accurately predict the startup critical hydraulic gradient of sandy soil fine particles.

**Keywords:** seepage; suffusion; fine particle loss; onset of migration of fine particles; critical hydraulic gradient; DEM-CFD coupling

### 1 Introduction

Different from silt and clayey soil with small particle size and uniform distribution, the sandy soil with a wide range of particle size distribution may show the migration and loss of fine particles which flow through the soil matrix formed by coarse particles without destroying the soil structure under the seepage<sup>[1]</sup>. This phenomenon is called suffusion<sup>[2]</sup>. The soil with potential suffusion is internally unstable<sup>[3]</sup>. Under the groundwater seepage condition, the seepage damage caused by the suffusion of internally unstable sandy soil will affect the performance of geotechnical structures or foundations, such as dams, embankments and railway subgrade<sup>[4–5]</sup>.

The possibility of internal instability of sandy soil depends on particle gradation, particle shape, pore structure, etc., which is called geometric condition at the beginning of the instability. The hydraulic gradient and the resulted effective stress are called the initial hydraulic conditions<sup>[6]</sup>. Suffusion will begin when the soil satisfies both geometric and hydraulic conditions. The loss process of fine particles under suffusion can be divided into two stages: (1) the startup stage—the fine particles break away from the soil skeleton and no longer transfer stress; (2) the migration stage—the fine particles separate from the soil skeleton and

move into the pore network with the seepage water flow.

In terms of geometric conditions, Kézdi<sup>[7]</sup>, Kenney et al.<sup>[8]</sup> and Indraratna et al.<sup>[9]</sup> put forward the evaluation methods and standards of soil internal stability, which have been verified by a large number of theoretical, experimental research and engineering practice. In terms of hydraulic conditions, Indraratna et al.<sup>[10]</sup> proposed a theoretical model for the migration and loss of fine particles in soil along the pore channel based on the concept of equivalent pore diameter. Wang et al.<sup>[11]</sup> obtained the formula for calculating the critical hydraulic gradient of fine particles according to the ultimate stress balance of fine particles in the pore channel. According to the limit moment equilibrium condition of fine particles rolling around fixed particles, Huang et al.<sup>[12]</sup> obtained the formula for calculating the critical hydraulic gradient of fine particles in soil by rolling mode. Chang et al.<sup>[13]</sup> carried out seepage tests, and found that under initial conditions, the startup hydraulic gradient is smaller than that of seepage failure hydraulic gradient, and both increase with the increase of confining pressure. Liang et al.<sup>[14]</sup> defined the low and high critical hydraulic gradient corresponding to the local movement and global loss of fine particles based on the seepage test. Li et al.<sup>[6]</sup> considered the stress reduction and took the zero effective stress state of fine

Received: 23 August 2019

Revised: 16 December 2019

This work is supported by the General Program of National Natural Science Foundation of China (51878568).

First author: WANG Ming-nian, male, born in 1965, PhD, Professor, PhD supervisor, mainly engaged in teaching and scientific research related to tunnels and underground engineering. E-mail: 19910622@163.com

Corresponding author: YU Li, female, born in 1978, PhD, Associate Professor, Doctoral supervisor, mainly engaged in teaching and scientific research related to tunnels and underground engineering. E-mail: yuli\_1026@home.swjtu.edu.cn

particles as the soil seepage failure condition, and obtained the hydraulic gradient calculation formula of seepage failure. Israr et al.<sup>[15]</sup> introduced stress reduction coefficient and considered the friction between soil particles, then established the theoretical model of soil seepage failure. Meanwhile, they gave the corresponding formula for calculating hydraulic gradient of soil seepage failure.

At present, scholars have done a lot of research on the migration process of fine particles in soil pore network and hydraulic gradient of seepage failure, however, there is no research on the effects of effective stress on fine particles in the migration startup process.

In order to solve the problem of suffusion of internally unstable sandy soil under the seepage, a model that can calculate the force acted on internally unstable soil under seepage is established in this paper from the point of view of fine particle startup, combined with soil effective stress and stress reduction on fine particles. The idea and method for calculating the force acted on fine particles are given, and the critical hydraulic gradient of fine particles is put forward for the first time. The formula for calculating the critical hydraulic gradient of fine particles in sandy soil is derived according to the ultimate stress equilibrium state, which provides the basis for quantitative analysis of the hydraulic conditions for the migration of fine particles. According to the calculation formula, the variation of critical hydraulic gradient of fine particles with buried depth is obtained. The verification of DEM-CFD coupling method and existing experimental data shows that the formula can accurately predict the startup critical hydraulic gradient of fine particles migration in sandy soil.

## 2 Stress analysis of fine particles

### 2.1 Effective stress on fine particles under the seepage

Skempton et al.<sup>[16]</sup> proposed the concept of critical fine particle content. If the fine particle content is less than the critical fine particle content, the fine particles can't fill the pores between the coarse particles. At this time, the fine particles bear relatively low stress and may move under the seepage force, which is called an internally unstable soil<sup>[17]</sup>. In order to quantify this effect, Skempton suggested a stress reduction coefficient  $\alpha$ , which is defined as the ratio of the stress transmitted by fine particles to the effective stress of the overburden.

As shown in Fig. 1, the buried depth of the soil element  $S$  is  $H$ , and area is  $a$ , which are taken from the sandy soil affected by seepage (hydraulic gradient  $i$ , seepage direction  $\theta$ ). Considering stress reduction for fine particles, the dead weight of overlying soil is  $\alpha\gamma'aH$ , and under the seepage, the seepage force<sup>[18]</sup> of overlying soil is  $i\gamma_w aH \sin \theta$ . The equilibrium state of vertical stress of the soil element is

$$[\sigma_{ij}'] = \begin{pmatrix} \sigma_m & \tau_{mn} \\ \tau_{nm} & \sigma_n \end{pmatrix} = \begin{pmatrix} \sigma'_{x,\text{fine}} \cos^2 \beta + \sigma'_{y,\text{fine}} \sin^2 \beta & \sin \beta \cos \beta (\sigma'_{y,\text{fine}} - \sigma'_{x,\text{fine}}) \\ \sin \beta \cos \beta (\sigma'_{y,\text{fine}} - \sigma'_{x,\text{fine}}) & \sigma'_{x,\text{fine}} \sin^2 \beta + \sigma'_{y,\text{fine}} \cos^2 \beta \end{pmatrix} \quad (6)$$

$$\alpha\gamma'aH - i\gamma_w aH \sin \theta = a\sigma'_{y,\text{fine}} \quad (1)$$

where  $\alpha$  is the stress reduction coefficient;  $\gamma'$  is the buoyant unit weight of the soil;  $a$  is the area of the soil element;  $H$  is the buried depth of the fine particles;  $i$  is the hydraulic gradient;  $\gamma_w$  is the unit weight of the water;  $\theta$  is the seepage direction; and  $\sigma'_{y,\text{fine}}$  is the vertical effective stress transmitted by the fine particles.

The vertical effective stress transmitted by fine particles can be obtained:

$$\sigma'_{y,\text{fine}} = (\alpha\gamma' - i\gamma_w \sin \theta)H \quad (2)$$

The horizontal effective stress of fine particles is

$$\sigma'_{x,\text{fine}} = K_0 \sigma'_{y,\text{fine}} \quad (3)$$

where  $K_0$  is the lateral pressure coefficient of the soil, for sandy soil<sup>[19]</sup> there is  $K_0 = 1 - \sin \phi'$ ; and  $\phi'$  is the effective internal friction angle of the soil.

For the internally unstable soil, when the fine particles are eroded, the effective stress carried by the fine particles is 0, namely,

$$\sigma'_{y,\text{fine}} = 0 \quad (4)$$

The corresponding hydraulic gradient can be obtained:

$$i_c = \frac{\alpha\gamma'}{\gamma_w \sin \theta} \quad (5)$$

where  $i_c$  is the hydraulic gradient of seepage failure of internally unstable soil proposed by Skempton et al.

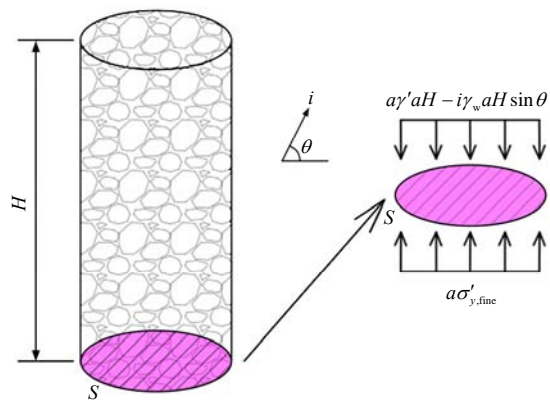


Fig. 1 Stress balance of soil element under seepage action

### 2.2 Force of fine sandy soil particles under seepage

As shown in Fig. 2, regarding the soil as a continuous, uniform and isotropic material, the  $xoy$  coordinate system is rotated counterclockwise around the  $o$ -point at any angle  $\beta$  to obtain the “ $mon$ ” coordinate system, and the stress components in the “ $mon$ ” coordinate system are<sup>[20]</sup>

where  $\sigma_m$  and  $\sigma_n$  are the normal stresses on  $m$  and  $n$  planes (normal directions of planes are parallel to  $m$  and  $n$  axes, respectively), respectively;  $\tau_{nm}$  is the tangential stress on  $m$ -plane pointing to  $n$ -plane; and  $\tau_{mn}$  is the tangential stress on  $n$ -plane pointing to  $m$ -plane.

Under the seepage, the gravity of fine particles is  $G$  [18]

$$G = \frac{\pi d^3 \gamma' (1 + e)}{6} \quad (7)$$

where  $d$  is the particle size;  $\gamma'$  is the buoyant unit weight of the soil; and  $e$  is the void ratio. The supporting force  $N$  of the fine particles in equilibrium with the dead weight can be decomposed into  $N_m$  and  $N_n$  along the  $m$  and  $n$  axes, respectively in the  $mon$

coordinate system.

As shown in Fig. 3, it can be considered that the force acted on fine particles consists of two parts, i.e., the effective stress in the soil, and the dead weight and the supporting force in equilibrium. The forces acted on the fine particles by the surrounding particles are combined into the contact force acted at the four intersections of the  $m$ -axis and  $n$ -axis parallel lines passing through the center of the particles and the surface of the particles. The contact force can be calculated by integrating the area of action with the corresponding stress component and adding the supporting force component:

$$F_i = \int_s \left( \frac{\sigma_i}{1 - e} \right) ds + N_i \quad (8)$$

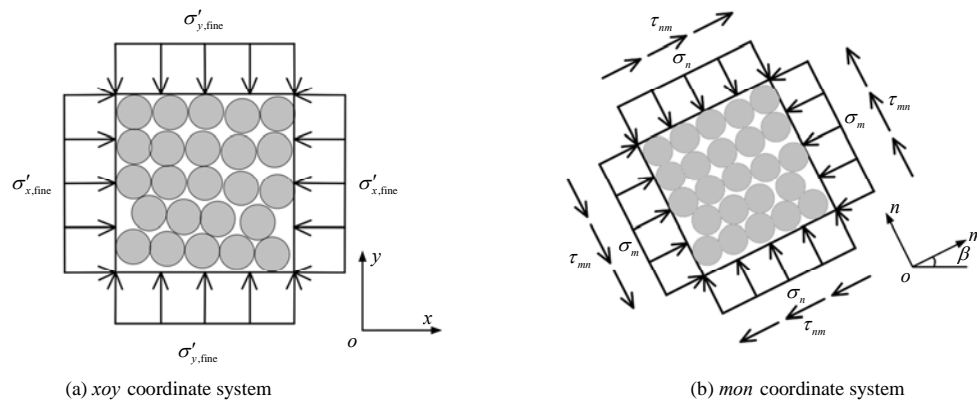


Fig. 2 Effective stress of soil mass

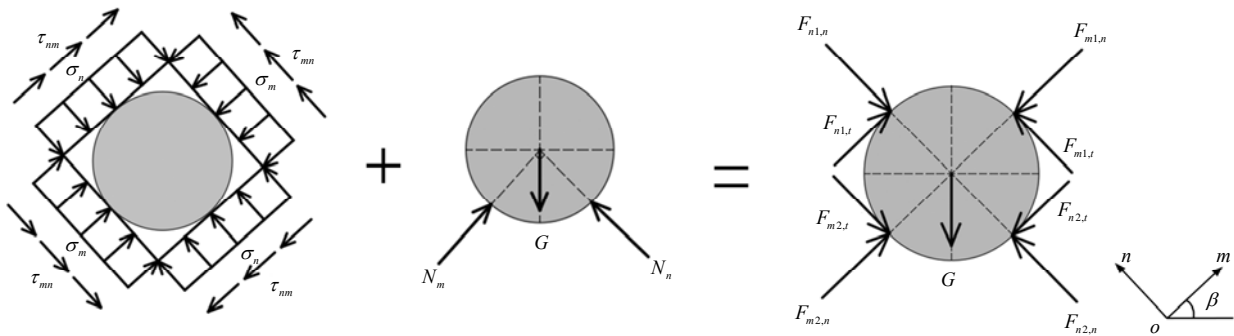


Fig. 3 Stress analysis of fine particles

where  $F_i$  is the  $i^{\text{th}}$  contact force;  $\sigma_i$  is the stress component corresponding to the  $i^{\text{th}}$  contact force;  $s$  is the area of the stress component that acted on, which is  $\pi d^2 / 4$ ; and  $N_i$  is the supporting force component corresponding to the  $i^{\text{th}}$  contact force.

Under the seepage, fine particles are affected by the seepage force due to pore water flow, and the seepage velocity is very small. Ignoring the change of dynamic water head, the seepage force on a single particle is [18]

$$F = \frac{1}{6} \pi d^2 \gamma_w i (d + e d_{\theta k}) \quad (9)$$

where  $d_{\theta k}$  is the equivalent size of soil particle,  $d_{\theta k} = 1 / \sum (p_i / d_i)$ ; and  $p_i$  is the percentage content of soil particles with particle size of  $d_i$ .

Under the seepage condition, the force acted on fine particles is shown in Fig. 4.

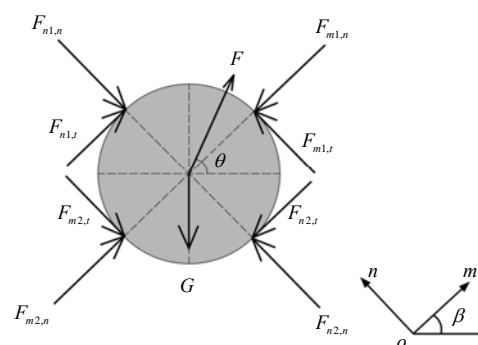


Fig. 4 Stresses acted on a fine particle under seepage action

### 3 Startup critical hydraulic gradient of fine particles

#### 3.1 Geometric conditions of fine particle startup migration

At present, scholars have proposed a variety of soil internal stability evaluation criteria<sup>[7-9]</sup> to judge the occurrence of suffusion. For example, Kenney et al.<sup>[8]</sup> thought that when  $(F / H)_{\min} > 1$ , fine particles can fill the pores between coarse particles, and suffusion will not occur (for particles with arbitrary particle size,  $F$  is the mass fraction of soil particles with particle size of  $0-d$ ;  $H$  is the mass fraction of soil particles with particle size of  $d-4d$ ).

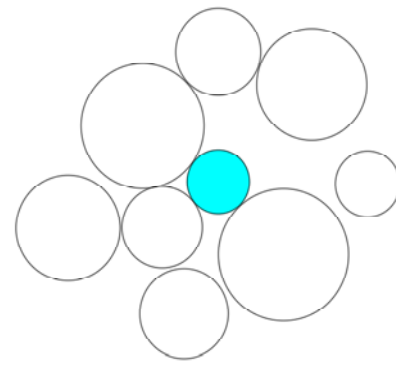
As shown in Fig.5(a), there are different entrances and exits of the pores between particles, and these openings form a “constriction” along the flow path through the material; and for a single fine particle, there is a series of pores and constriction of different sizes around. The diameter of the largest sphere which can pass through the collar stuck is called the collar stuck size. When the fine particle size is larger than the adjacent collar stuck size in the potential startup direction, the fine particle can’t start, if it is smaller than the collar stuck size, suffusion may occur.

With the increase of hydraulic gradient, the fine particles that meet the geometric conditions to startup will eventually migrate. As shown in Fig. 5(b), it can be considered that the fine particles are located at the startup point of the pore channel. If the fine particles overcome the contact force of the surrounding particles under the seepage force, they will break away from the soil skeleton and no longer transfer stress, that is, the fine particles will start migrate. At this time, there are two potential startup modes of fine particles: rolling and sliding.

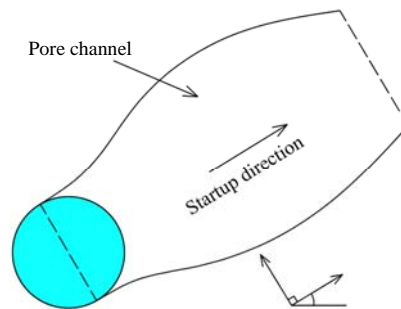
#### 3.2 Rolling

As shown in Fig. 6(a), when fine particles start rolling, there are two possibilities: rolling around the upper contact point  $M$  and rolling around the lower contact point  $N$ . Take the rolling startup around the lower contact point  $N$  as an example.

Under dry condition, the fine particles located at the startup point of the pore channel, (angle between the pore channel and the horizontal direction is  $\beta$ ), are no longer affected by  $F_{m1,n}, F_{m1,t}, F_{m2,n}, F_{m2,t}$ ; and the normal contact forces perpendicular to the pore channel  $F_{n1,n}$  and  $F_{n2,n}$  remain unchanged, while the tangential contact forces  $F_{n1,t}$  and  $F_{n2,t}$  are adjusted. Under the seepage condition, the normal contact forces of fine particles at two contact points are expressed as  $F_{Mn}$  and  $F_{Nn}$ , and the tangential contact forces are  $F_{Mt}$  and  $F_{Nt}$ . In this case, the normal contact force on both sides of the pore channel is redistributed, and it is assumed that the penetration force component perpendicular to the pore channel is borne by the normal contact force on both sides of the pore channel, we can get

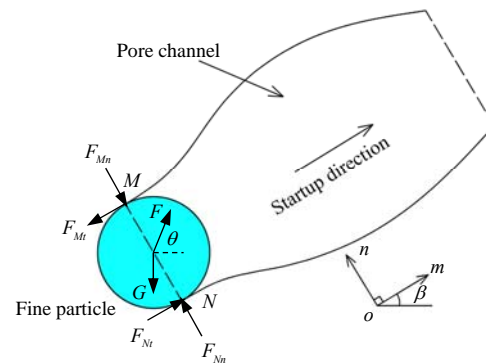


(a) Particle distribution

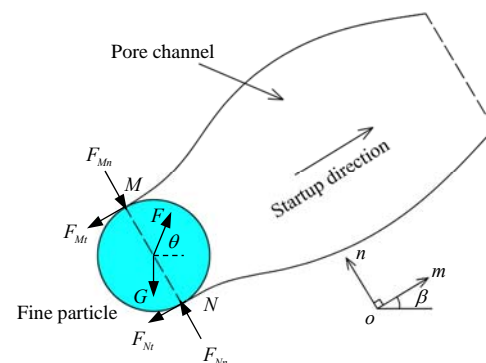


(b) Pore channel

Fig. 5 Particle distribution and migration loss channels



(a) Rolling



(b) Sliding

Fig. 6 Initiation of fine particle migration

$$\left. \begin{aligned} F_{Mn} &= F_{n1,n} + \frac{F \sin(\theta - \beta)}{2} \\ F_{Nn} &= F_{n2,n} - \frac{F \sin(\theta - \beta)}{2} \end{aligned} \right\} \quad (10)$$

where  $F_{Mn}$  and  $F_{Nn}$  are the normal contact forces at  $M$  and  $N$  points, respectively; and  $F$  is the penetration force on fine particles.

The tangential contact force is

$$\left. \begin{aligned} F_{Mt} &= F_{Mn} \tan \varphi' \\ F_{Nt} &= F_{Nn} \tan \varphi' \end{aligned} \right\} \quad (11)$$

$$i_{rN} = \begin{cases} \frac{3\alpha\gamma'H(1 - \sin^2\beta) \tan\varphi' + \gamma'(1 - e^2)d \sin\beta}{3\gamma_w H \sin\theta(1 - \sin^2\beta) \tan\varphi' + \gamma_w(1 - e)(d + ed_{ok})[\cos(\theta - \beta) - \tan\varphi' \sin(\theta - \beta)]} & \beta \subseteq [0^\circ, 90^\circ] \cup [270^\circ, 360^\circ] \\ \frac{3\alpha\gamma'H(1 - \sin^2\beta) \tan\varphi' + \gamma'(1 - e^2)d(\sin\beta - 2 \tan\varphi' \cos\beta)}{3\gamma_w H \sin\theta(1 - \sin^2\beta) \tan\varphi' + \gamma_w(1 - e)(d + ed_{ok})[\cos(\theta - \beta) - \tan\varphi' \sin(\theta - \beta)]} & \beta \subseteq [90^\circ, 270^\circ] \end{cases} \quad (13)$$

Similarly, the hydraulic gradient of fine particles rolling around the upper contact point  $M$  in sandy soil can be obtained as follows:

$$i_{rM} = \begin{cases} \frac{3\alpha\gamma'H(1 - \sin^2\beta) \tan\varphi' + \gamma'(1 - e^2)d(\sin\beta + 2 \tan\varphi' \cos\beta)}{3\gamma_w H \sin\theta(1 - \sin^2\beta) \tan\varphi' + \gamma_w(1 - e)(d + ed_{ok})[\cos(\theta - \beta) + \tan\varphi' \sin(\theta - \beta)]} & \beta \subseteq [0^\circ, 90^\circ] \cup [270^\circ, 360^\circ] \\ \frac{3\alpha\gamma'H(1 - \sin^2\beta) \tan\varphi' + \gamma'(1 - e^2)d \sin\beta}{3\gamma_w H \sin\theta(1 - \sin^2\beta) \tan\varphi' + \gamma_w(1 - e)(d + ed_{ok})[\cos(\theta - \beta) + \tan\varphi' \sin(\theta - \beta)]} & \beta \subseteq [90^\circ, 270^\circ] \end{cases} \quad (14)$$

### 3.3 Sliding

As shown in Fig. 6(b), when the fine particles start in a sliding manner, the force is balanced along the direction of the pore channel:

$$F \cos(\theta - \beta) - G \sin\beta - F_{Mt} - F_{Nt} = 0 \quad (15)$$

By solving all equations simultaneously, the startup hydraulic gradient initiated by sliding of fine particles in sandy soil can be obtained as follows:

$$i_s = \begin{cases} \frac{3\alpha\gamma'H(1 - \sin^2\beta) \tan\varphi' + \gamma'(1 - e^2)d(\sin\beta + \tan\varphi' \cos\beta)}{3\gamma_w H \sin\theta(1 - \sin^2\beta) \tan\varphi' + \gamma_w(1 - e)(d + ed_{ok})\cos(\theta - \beta)} & \beta \subseteq [0^\circ, 90^\circ] \cup [270^\circ, 360^\circ] \\ \frac{3\alpha\gamma'H(1 - \sin^2\beta) \tan\varphi' + \gamma'(1 - e^2)d(\sin\beta - \tan\varphi' \cos\beta)}{3\gamma_w H \sin\theta(1 - \sin^2\beta) \tan\varphi' + \gamma_w(1 - e)(d + ed_{ok})\cos(\theta - \beta)} & \beta \subseteq [90^\circ, 270^\circ] \end{cases} \quad (16)$$

### 3.4 Startup critical hydraulic gradient

Fine particles will start to move when the hydraulic gradient meet any startup mode. By comparison, it is found that the startup hydraulic gradient required for fine particles rolling is less than that of the startup hydraulic gradient of sliding, indicating that fine particles in sandy soil will generally start by rolling. As a kind of critical hydraulic gradient, the hydraulic gradient corresponding to fine particle migration startup is called startup critical hydraulic gradient in this paper.

The minimum hydraulic gradient required in different startup modes is taken as the critical hydraulic gradient for fine particles to start:

$$i_q = \min(i_{rN}, i_{rM}, i_s) \quad (17)$$

where  $i_{rN}$  is hydraulic gradient when the fine particles startup in rolling around the contact point  $N$ , and  $i_{rM}$  is the hydraulic gradient when fine particles startup in rolling around the contact point  $M$ .

The critical hydraulic gradient of fine particles in sandy soil is

$$i_q = \frac{3\alpha\gamma'H(1 - \sin^2\beta) \tan\varphi' + \gamma'(1 - e^2)d(\sin\beta + 2 \tan\varphi' |\cos\beta|)}{3\gamma_w H \sin\theta(1 - \sin^2\beta) \tan\varphi' + \gamma_w(1 - e)(d + ed_{ok})[\cos(\theta - \beta) + \tan\varphi' |\sin(\theta - \beta)|]} \quad (18)$$

Equation (18) shows that when the buried depth is shallow, the critical hydraulic gradient of fine particles in sandy soil is not only related to seepage flow (hydraulic gradient, seepage direction) and soil characteristics (stress reduction coefficient, buoyancy unit weight, effective internal friction angle, void ratio, equivalent

particle size). It is also affected by the buried depth and particle size. At the same time, the startup critical hydraulic gradients of fine particles in different directions are also different.

When the buried depth is large ( $H \gg d$ ), the Eq. (18) can be simplified to

$$i_q = \frac{\alpha \gamma'}{\gamma_w \sin \theta} \quad (19)$$

Equation (19) is the commonly used hydraulic gradient of seepage failure at present, which suggests that the critical hydraulic gradient of fine particles has nothing to do with the characteristics of particles and is controlled by soil buoyancy unit weight, stress reduction coefficient and seepage flow.

### 4 Results and discussion

Different from the previous understanding, according to the formula for calculating the critical hydraulic gradient of fine particles, the hydraulic gradient of fine particles under the seepage is not only related to seepage flow, soil characteristics and particle size, but also affected by the buried depth of fine particles. According to the formula for calculating the critical hydraulic gradient of fine particles, this section analyzes

the critical hydraulic gradient of fine particles in different buried depths of sandy soil samples under the upward seepage flow condition, and discusses the effect of the buried depth of fine particles on the critical hydraulic gradient.

#### 4.1 Physical and mechanical parameters of sandy soil samples

The filter consists of the coarse component and the fine component from the sandy soil sample. The coarse component is coarse sand with particle size 0.5–2.0mm, and the PSD curve and the constriction size distribution (CSD) curve are shown in Fig. 7. Fine particles with particle sizes of 0.1, 0.2 and 0.3 mm were used as fine component to form sandy soil samples. The stress reduction coefficient of sandy soil sample is determined according to the method from Israr et al.<sup>[15]</sup>, and the physical and mechanical parameters of soil sample are shown in Table 1.

**Table 1 Physical and mechanical properties of soil samples**

Sample number	Density $\rho$ / (kg · m <sup>-3</sup> )	Void ratio $e$	Buoyant unit weight $\gamma'$ / (N · m <sup>-3</sup> )	Average diameter $d_{ok}$ / mm	Stress reduction coefficient $\alpha$	Effective internal friction angle $\varphi'$ / (°)	Hydraulic gradient at failure state
1	1 720	0.821	11 710	0.623	0.174		0.194
2	1 820	0.739	12 450	0.688	0.745	30	0.928
3	1 820	0.757	12 510	0.819	1.000		1.251

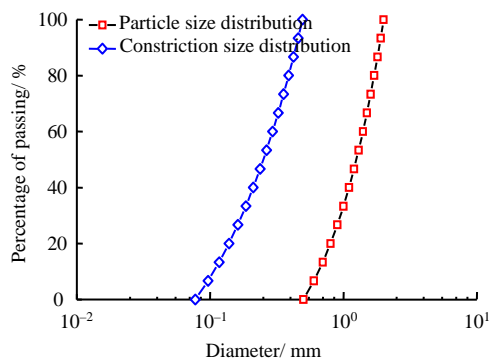


**Fig. 7 Coarse particle size distribution and CSD curves**

#### 4.2 Critical startup hydraulic gradient of fine particles under upward seepage

Soil sample 2 with fine particle size of 0.2 mm is taken as an example. Under the vertical seepage, the critical hydraulic gradient of fine particles with different burial depths is calculated as shown in Fig. 8.

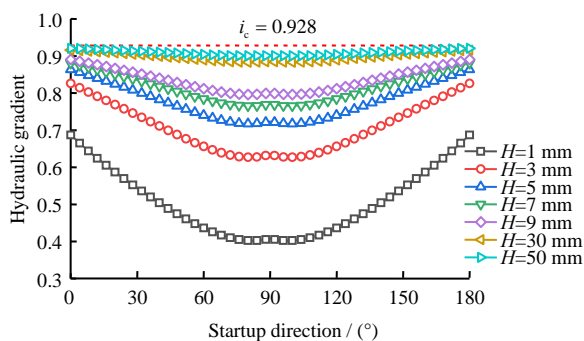


**Fig. 8 Startup critical hydraulic gradient of fine particles with different buried depths**

It can be seen from Fig. 8 that there are differences in the critical hydraulic gradient of fine particles starting in different directions. With the increase of buried depth, the critical hydraulic gradient of fine particles increases gradually and approaches to the hydraulic gradient of seepage failure.

The ratio of the difference between the highest and lowest startup critical hydraulic gradient of fine particles in the same buried depth in different directions and the lowest startup critical hydraulic gradient is defined as the coefficient of variation, namely

$$\delta = \frac{i_{q,max} - i_{q,min}}{i_{q,min}} \quad (20)$$

where  $\delta$  is the coefficient of variation;  $i_{q,max}$  is the highest startup critical hydraulic gradient; and  $i_{q,min}$  is the lowest startup critical hydraulic gradient.

The highest and lowest startup critical hydraulic gradient and coefficient of variation of fine particles are shown in Fig. 9. It can be seen from the figure that with the increase of buried depth, the critical hydraulic gradient of fine particles is gradually close to the hydraulic gradient of seepage failure. At the same time, the difference between the highest and lowest critical hydraulic gradient of fine particles decreases gradually, and the coefficient of variation is 0.101 69 when the buried depth is 1 cm. The coefficient of variation is 0.052 165 when the buried depth is 2 cm. and the coefficient of variation is 0.010 61 when the buried depth is 10 cm.



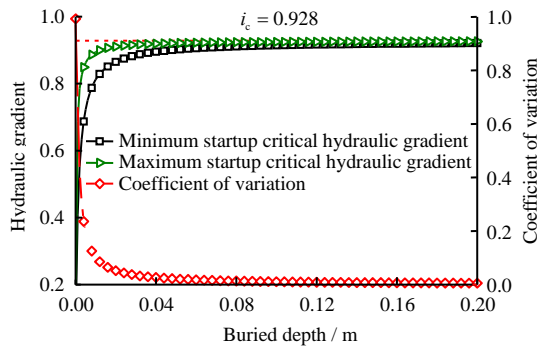


Fig.9 Minimum and maximum startup critical hydraulic gradient and coefficient of variation

5 Formula verification

5.1 DEM-CFD coupled simulation verification

At present, the DEM-CFD coupled simulation method

has been widely used in the field of geotechnical and underground engineering. The DEM-CFD coupled simulation method is used to simulate the seepage of internally unstable sandy soil, and the formula for calculating the critical hydraulic gradient of fine particles is verified. The solid phase and liquid phase simulations are carried out by using the discrete element (DEM) software PFC3D and the computational fluid dynamics (CFD) software OpenFOAM, respectively.

From the previous section, it is known that the critical hydraulic gradient of fine particles in the surface layer of sandy soil (buried depth is less than 1cm) is greatly affected by buried depth. Considering the calculation efficiency, the size of sandy soil model is 1cm × 1cm × 1cm. Physical and mechanical parameters are selected as shown Table 1. The PFC model parameters are shown in Table 2.

Table 2 PFC model parameters

Sample number	Fine particle diameter / mm	Fine particle content / %	Coarse particle diameter / mm	Number of particles	Density / (kg · m <sup>-3</sup> )	Modulus / MPa	Stiffness ratio	Friction coefficient
1	0.1	8	0.5~2.0	60 666	3 600	1	1	0.4
2	0.2	14	0.5~2.0	15 872	3 600	1	1	0.4
3	0.3	14	0.5~2.0	5 885	3 600	1	1	0.4

The PFC model and flow field for soil sample 2 are shown in Fig. 10.

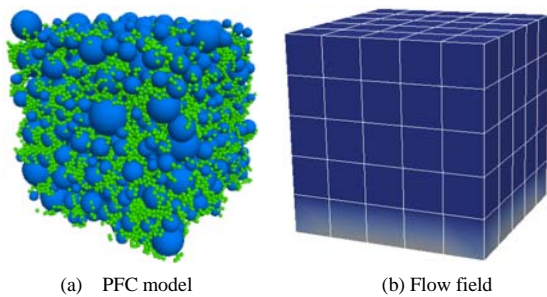


Fig.10 PFC model and flow field

In the simulation process, an increasing vertical upward hydraulic gradient is applied to the sandy soil sample, and the migration and loss state of fine particles under different hydraulic gradient is shown in Fig. 11.

Figure11(a) that when the hydraulic gradient  $i=0$ , the fine particles in the soil sample basically remain constant. A small number of fine particles change their locations and the particles start to move as illustrated in Fig.11(b) when the hydraulic gradient  $i=0.4$ . It is seen most of the fine particles change their locations and migrate and move under the seepage (Fig. 11(c)) when the hydraulic gradient  $i=0.8$ . As can be seen from Fig. 11(d), when the hydraulic gradient  $i=1.3$ , both coarse and fine particles begin to move, and the soil sample is damaged by uplift.

The sandy soil sample is divided into five layers vertically from top to bottom, and the displacement

and quantity of fine particles in each layer are monitored during the simulation process. If the fine particles can move to the adjacent pores through the constriction, the startup occurs.  $d_{th} / 2$  is taken as the startup critical value of displacement of fine particles, and when the displacement of fine particles is greater than the critical value, the startup of fine particles is considered. The change of the number of fine particles in each layer is shown in Fig. 12, and the change in the startup number of fine particles is shown in Fig. 13.

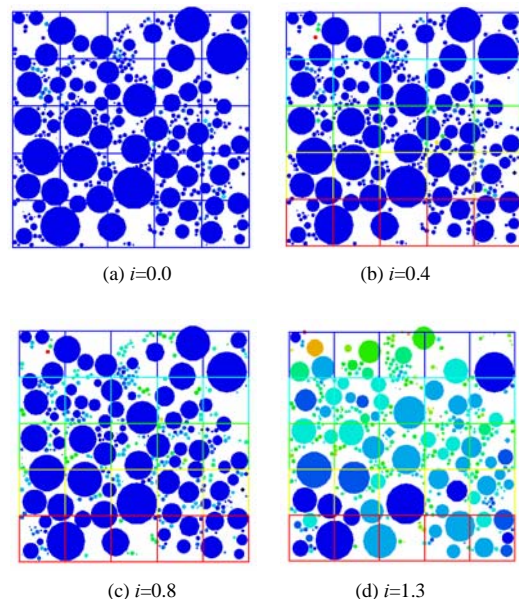


Fig. 11 Fine particle migration and particle loss under seepage

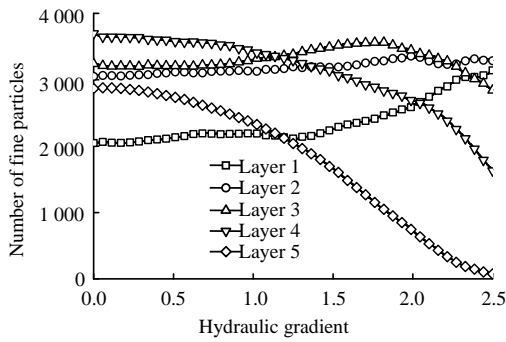


Fig. 12 Number of fine particle changes

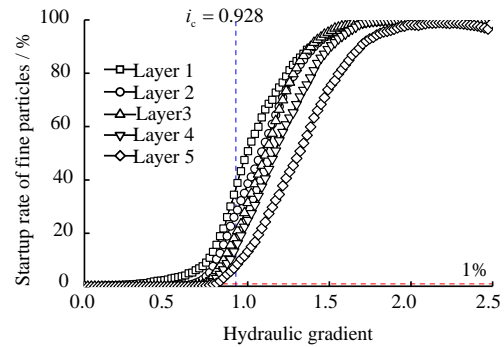


Fig. 14 Startup rate of fine particles

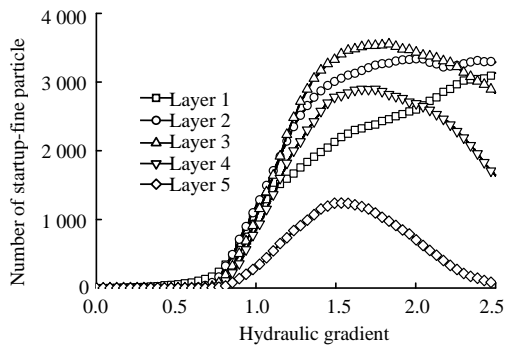


Fig. 13 Number of startup-fine particle changes

It can be seen from Fig. 12 that under the seepage, the number of fine particles in the bottom fourth and fifth layers of the soil sample decreases continuously, and under the supplement of fine particles lost in fourth and fifth layers, the number of fine particles in the second and third layers changes little. As the number of fine particles migrate to the first layer, the number of fine particles in the first layer increases gradually. As shown in Fig. 13, with the increase of the hydraulic gradient, the number of migrated fine particles in layers 1–5 increased, and the number of moved fine particles increases gradually with the increased of hydraulic gradient.

After the initial equilibrium, there are suspended particles in the model which do not transfer stress, and the suspended particles may start moving when the hydraulic gradient is very small. We found that in the initial stage of seepage, the startup rate of fine particles (the ratio of the number of fine particles to the total amount of fine particles) changed abruptly with the increase of hydraulic gradient, and when the startup rate of fine particles reached 1%, it basically changed with the law of hydraulic gradient. In order to eliminate the impact of suspended particles, the hydraulic gradient corresponding to the startup of 1% of fine particles in each layer is taken as the lowest startup critical hydraulic gradient of fine particles, and the startup rate of fine particles in each layer varies with the hydraulic gradient as shown in Fig. 14.

As can be seen from Fig. 14, under the seepage, the startup rate of fine particles in layers 1–5 has reached 1% successively, and with the increase of hydraulic gradient, the fine particles in each layer are basically started.

The minimum startup critical hydraulic gradient of fine particles obtained by calculation formula and numerical simulation is shown in Fig. 15, and the calculation results of the formula are basically consistent with the results of numerical simulation.

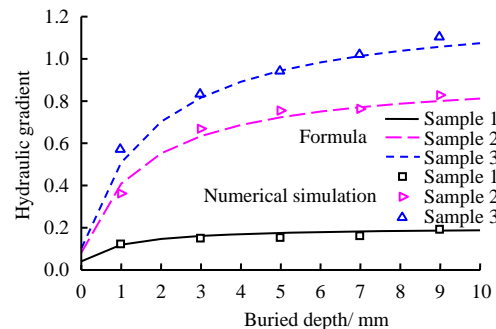


Fig. 15 Minimum startup critical hydraulic gradient

The comparison of the minimum startup critical hydraulic gradient of fine particles obtained by the calculation formula and numerical simulation is shown in Fig. 16. The data points are basically distributed along the isoline, and the maximum standard error is 6.038%, deviation is within 6%.

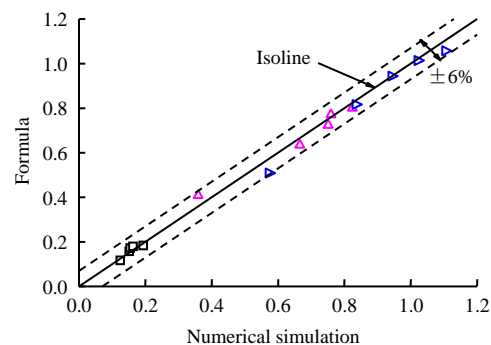


Fig. 16 Comparison of model and numerical simulations

## 5.2 Model validation with existing test data

Israr et al.<sup>[15]</sup> carried out permeability tests on granular soils with different relative densities, and the variation of effluent turbidity and flow velocity with hydraulic gradient is plotted in Fig. 17.

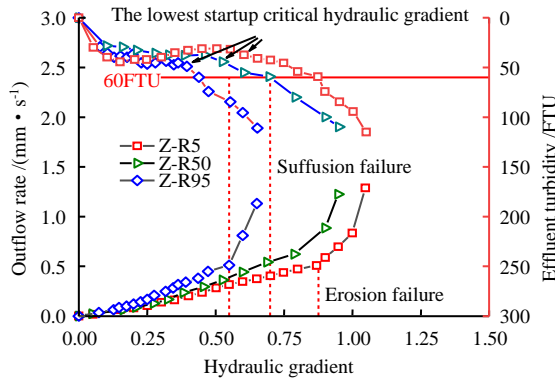


Fig. 17 Effluent turbidity and flow velocity variations versus hydraulic gradient

Figure 17 presents that the turbidity of the effluent

keeps a low value at the beginning of seepage, indicating that the suspended particles in the soil will be lost with the water flow after the beginning of seepage. With the increase of hydraulic slope, the turbidity of effluent suddenly begins to increase rapidly under a critical hydraulic gradient, corresponding to the lowest startup critical hydraulic gradient of fine particles in the surface layer. The hydraulic gradient continues to increase, and when the effluent turbidity reaches 60FTU, the effluent velocity increases suddenly, and the seepage failure occurs in the soil sample, which corresponds to the failure hydraulic gradient.

The minimum startup critical hydraulic gradients of fine particles in the surface layer (The soil equivalent particle size is taken as the burial depth of surface fine particles) obtained by Israr's test and calculation formula in this paper are shown in Table 3. Figure 18 shows the minimum startup critical hydraulic gradient of fine particles obtained by comparing the test data and the calculation formula, the data points are basically distributed along the isoline, and the maximum standard error is 11.211%, deviation is within 12%.

Table 3 Comparison between existing test data and model calculation results

Sample number	Buoyance unit weight $\gamma'$ / (kN · m <sup>-3</sup> )	Relative density $R_d$ / %	Fine particle content / %	Void ratio	Stress reduction coefficient	Equivalent particle diameter $d_{0k}$ / mm	Equivalent fine particle diameter / mm	The lowest startup hydraulic gradient $i_{q,min}$	
								Experiment	Formula
Y-R5	9.4	7		0.925	0.40			0.362	0.355
Y-R50	10.4	53	30	0.680	0.44	3.95	0.250	0.422	0.391
Y-R95	11.4	97		0.447	0.51			0.484	0.488
Z-R5	9.5	5		0.867	0.53			0.391	0.453
Z-R50	10.4	51	20	0.628	0.64	1.83	0.100	0.525	0.543
Z-R95	11.3	94		0.405	0.75			0.602	0.687
U-R5	9.7	6		0.855	0.14			0.099	0.124
U-R50	10.6	54	19	0.607	0.17	0.45	0.001	0.153	0.153
U-R95	11.5	98		0.379	0.20			0.192	0.198

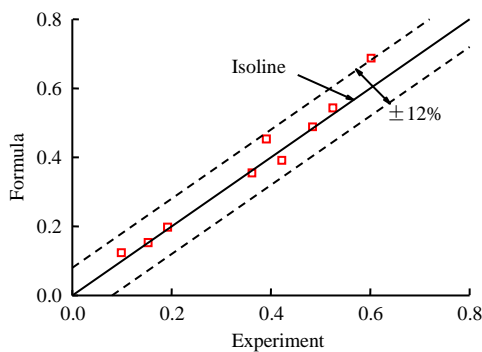


Fig. 18 Comparison between model prediction and experimental data

## 6 Conclusions

In order to investigate the startup of suffusion of internally unstable sandy soil, a formula for calculating the critical hydraulic gradient of fine particles in sandy soil is developed, and is verified by DEM-CFD coupled method and existing test results. The conclusions are as follows:

The formula for calculating the startup critical hydraulic gradient of fine particles in sandy soil is

derived according to the ultimate stress equilibrium state. The maximum standard errors are 6.038% and 11.211%, respectively with DEM-CFD coupled method and seepage test results, indicating that the formula can accurately predict the threshold hydraulic gradient of fine particles.

The startup critical hydraulic gradient of fine particles on the surface of sandy soil is greatly affected by the buried depth. With the increase of buried depth, the difference between the highest and lowest critical startup hydraulic gradient of fine particles decreases gradually and approaches to the hydraulic gradient of seepage failure. The difference between the highest and lowest startup critical hydraulic gradient is 10.169% when the buried depth is 1 cm, and the difference is 1.061% when the buried depth is 10cm.

Compared with the numerical simulation and test results, there are still some errors in the calculation formula. It is considered that there are mainly the following reasons.

(i) In the process of establishing the force balance model of fine particles, it is assumed that the soil is a continuous, uniform and isotropic material. The stress state of fine particles is obtained by the model, which

is different from the real stress state of fine particles.

(ii) Both the calculation formula and the DEM-CFD coupled method assume that the sandy soil particles are spheres and ignore the shape effect.

(iii) The formula for calculating the startup critical hydraulic gradient is derived from the limit force balance of fine particles, without considering the deformation of fine particles and the adjustment of the position between particles. The fine particles may not reach the equilibrium state of ultimate stress in reality.

(iv) The average hydraulic gradient is used in the calculation process, and the change of the local seepage state is not taken into account. The local hydraulic gradient usually changes with the location, and the practicability of the calculation formula needs to be further improved.

## References

- [1] HUNTER R P, BOWMAN E T. Visualisation of seepage-induced suffusion and suffosion within internally erodible granular media[J]. *Geotechnique*, 2018, 68(10): 918–930.
- [2] WU Meng-xi, YE Fa-ming, ZHANG Qi. Effect of fine grain loss on the stress-strain relationship of sand and gravel soils[J]. *Rock and Soil Mechanics*, 2017, 38(6): 1550–1556.
- [3] WU Meng-xi, GAO Gui-yun, YANG Jia-xiu, et al. A method of predicting critical gradient for piping of sand and gravel soils[J]. *Rock and Soil Mechanics*, 2019, 40(3): 861–870.
- [4] FELL R, WAN C F, CYGANIEWICZ J. Time for development of internal erosion and piping in embankment dams[J]. *Journal of Geotechnical and Geoenvironmental Engineering*, 2003, 129(4): 307–314.
- [5] BAO Xiao-hua, LIAO Zhi-guang, XU Chang-jie, et al. Model test study of the failure of silty sand slope under different seepage boundary conditions[J]. *Rock and Soil Mechanics*, 2019, 40(10): 3789–3796.
- [6] LI M, FANNIN R J. A theoretical envelope for internal instability of cohesionless soil[J]. *Geotechnique*, 2012, 62(1): 77–80.
- [7] KÉZDI A. Soil physics-selected topics-developments in geotechnical engineering-25[R]. Amsterdam: Elsevier, 1979.
- [8] KENNEY T, LAU D. Internal stability of granular filters[J]. *Canadian Geotechnical Journal*, 1985, 22(2): 215–225.
- [9] INDRARATNA B, NGUYEN V T, RUJIKIATKAMJORN C. Assessing the potential of internal erosion and suffusion of granular soils[J]. *Journal of Geotechnical and Geoenvironmental Engineering*, 2011, 137(5): 550–554.
- [10] INDRARATNA B, VAFAI F. Analytical model for particle migration within base soil-filter system[J]. *Journal of Geotechnical and Geoenvironmental Engineering*, 1997, 123(6): 600.
- [11] WANG Shuang, CHEN Jian-sheng, ZHONG Qi-ming. Study on critical hydraulic gradient of piping in granular soil[J]. *Journal of Hydropower Energy Science*, 2018, 36(9): 114–117.
- [12] HUANG Z, BAI Y C, XU H J. A theoretical model to predict the critical hydraulic gradient for soil particle movement under two-dimensional seepage flow[J]. *Water*, 2017, 9(11): 828.
- [13] CHANG Dong-Sheng, ZHANG Li-Min. Determination criteria of soil seepage stability[J]. *Rock and Soil Mechanics*, 2011, 32(1): 253–59.
- [14] LIANG Y, YEH T C J, ZHA Y Y. Onset of suffusion in gap-graded soils under upward seepage[J]. *Soils and Foundations*, 2017, 57(5): 849–860.
- [15] ISRAR J, INDRARATNA B. Study of critical hydraulic gradients for seepage-induced failures in granular soils[J]. *Journal of Geotechnical and Geoenvironmental Engineering*, 2019, 145(7): 04019025.
- [16] SKEMPTON A W, BROGAN J M. Experiments on piping in sandy gravels[J]. *Geotechnique*, 1994, 44(3): 449–460.
- [17] TO H D, TORRES S A G, SCHEUERMANN A. Primary fabric fraction analysis of granular soils[J]. *Acta Geotechnica*, 2015, 10(3): 375–387.
- [18] WU Liang-Ji. Calculation of critical slope of incohesive soil piping[J]. *Water Conservancy and Transportation Science Research*, 1980, 4(1): 90–95.
- [19] LI Guang-xin. Higher soil mechanics[M]. Beijing: Tsinghua University Press, 2004.
- [20] WANG Guang-qin, DING Gui-bao, YANG Jie. Elastic mechanics[M]. Beijing: Tsinghua University Press, 2015.